Chapter 1
Introduction

1.1. Introduction to Cavitation Phenomenon

Cavitation refers to a distinctive occurrence within liquid flows where there is a phase change process involving the rapid transformation of liquid into vapour in regions of low pressure, followed by collapsing or implosion when pressure rises again. The study of cavitation dates back to the late 19th century. While the term "cavitation" was originally coined by R. E. Froude and first documented by Barnaby and Thornycroft in 1895, the concept had been speculated upon much earlier by L. Euler in his 1754 theory on water turbines. However, the phenomenon of cavitation was initially observed and examined by Barnaby and Parsons in 1893. They identified that the formation of vapour bubbles on propeller blades had led to the failure of the sea trial of the British high-speed warship HMS Daring in 1885. In 1895, Parsons established the first water tunnel dedicated to cavitation research, revealing the connection between cavitation and propeller damage. The theoretical groundwork for cavitation research was laid by Rayleigh in 1917, as he successfully addressed the collapse of an empty cavity within a substantial liquid mass. Since then, numerous research work has been published on cavitating flow.

Cavitation is in nature a phase change process between liquid and vapour, which can be explained by using a pressure-temperature diagram presented in **Figure 1.1**. A substance, such as water, can undergo different phase changes based on the combination of pressure and temperature. Phase changes from liquid to vapour are commonly understood as vapourization, which can be achieved by boiling and cavitation. In contrast to boiling where the vapourization of liquid is

driven by a temperature change, cavitation could be approximated as an isothermal process starting when the local liquid pressure is reduced below its saturated vapour pressure P_{vap}, a value given by the tensile strength of the liquid at a certain temperature.

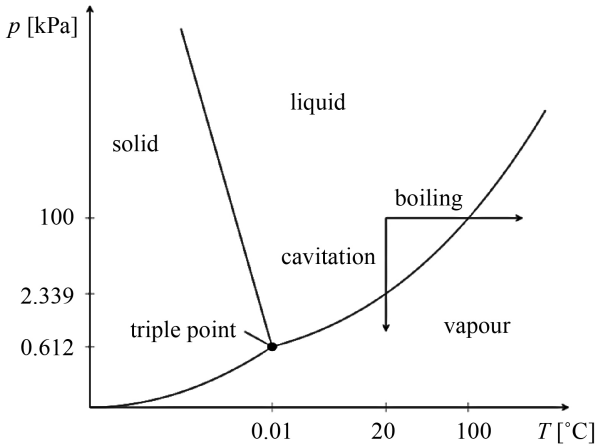

Figure 1.1. Pressure-temperature phase diagram of water.

It is important to note that pure water cannot cavitate even if the local pressure is under the vapour pressure since pure liquid water can resist very high tension until vapour cavities appear. Cavitation is generally initiated by cavitation nuclei. Their existence weakens cohesion of liquid molecules and thus serves as starting locations for liquid breakdown. The cavitation nuclei may be non-condensable gas bubbles in the bulk of water, or interfacial gaseous voids located on the surface of particles in the water, or on bounding walls (Mørch, 2015). These nuclei play a crucial role in initiating and promoting cavitation. When the pressure in the liquid drops below its vapour pressure, these nuclei act as sites for the rapid formation and growth of vapour bubbles. The cavitation nuclei content is a primary factor determining the difference between the vapour pressure and the ac-

tual pressure for cavitation inception (Franc & Michel 2005). Despite of the existence of this difference, the vapour pressure still serves as a quantity to assess macroscopic cavitation processes.

The presence and characteristics of cavitation nuclei influence the inception and behavior of cavitation in different fluid systems. For instance, the number, size, and distribution of nuclei can affect the intensity and extent of cavitation damage in hydraulic systems, pumps, and other fluid flow devices. Researchers and engineers study cavitation nuclei to understand and control cavitation effects and to design more efficient and durable engineering systems.

1.2. Thermodynamic Effects of Cavitation

Cavitation-induced vapour formation leads to the absorption of latent heat of evapouration from the nearby liquid, resulting in a reduction of local temperature and, consequently, the local vapour pressure surrounding the cavity. This phenomenon is referred to as a thermodynamic or thermal effect of cavitation. While this effect might not be significant in typical scenarios, such as when using water at room temperature, it becomes notably more consequential in the context of cryogenic fluids like liquid oxygen and liquid hydrogen. This thermodynamic impact of cavitation is particularly pronounced in applications involving cryogenic fluids. For instance, the performance of a turbopump inducer in a liquid propellant rocket engine benefits significantly when operating with cryogenic fluids compared to cold water. This is due to the suppression of cavity development caused by the localized reduction in vapour pressure resulting from the thermodynamic effect of cavitation.

The interest in investigating the thermodynamic effects of cavitation comes from manned space, deep space exploration, and other large aerospace activities. The increasing demand for liquid rocket high-thrust requirements would lead to a cryogenic fluid flowing

through the liquid carrier rocket propulsion systems propellant cavitation phenomenon, which can seriously affect the performance and reliability of the liquid carrier rocket. Therefore, accurate prediction of cryogenic cavitation is one of the key technologies for the high-thrust liquid rocket. In attempting to extrapolate the thermodynamic or thermal effects of cavitation from tests in cold water to cavitation in liquids with relatively high vapour pressures, such as light hydrocarbons and cryogenic fluids, where testing is impractical, dangerous, or expensive, scaling of thermal effects is very important. The early method to scale thermal effects in cavitating turbo pumps has been proposed by Stepanoff (1964). The thermal cavitation criterion B is used merely as an index of the "tendency" of the liquid to boil orits "readiness" to flash into vapour.

Efforts have been made to quantify the temperature drop in cavitation using fluid and vapour properties at a given temperature. The benchmark quantities for evaluating cavitation thermodynamic effects can be summarized with references as: (1) the B-factor, B, proposed by Stepanoff (1964) and improved by Ruggeri &Moore (1969); (2) the Jakob number, Ja, which is a reciprocal of the B-factor mathematically (Colombet *et al*. 2017; Franc *et al*. 2010); (3) the thermodynamic parameter, Σ, derived considering the Rayleigh-Plesset equations of bubble dynamics by Brennen (1973); (4) the C-factor, C, which involves the effects of flow velocity by Chen *et al*. (2017).

These scaling parameters provided above were mostly selected based on either single bubbly dynamics or heat balance at steady-state and can reasonably estimate the local temperature drop. As indicated by Utturkar *et al*. (2005), their applicability needs to be validated with experiments considering the complex cavitating flow environment.

1.3. Classification of Cavitation

Cavitation can be classified, according to vapour generation mechanisms, into

Acoustic cavitation: When acoustic waves propagate through a liquid, they create alternating regions of high and low pressure. In the regions of low pressure, small gas bubbles present in the liquid can expand and form cavitation bubbles. As the pressure fluctuates rapidly, these bubbles grow during low-pressure phases and violently collapse during high-pressure phases. It is a type of cavitation that is specifically triggered by acoustic energy. Acoustic cavitation finds applications in different fields. In medical applications, focused ultrasound waves can be used to generate cavitation bubbles for procedures like lithotripsy. In cleaning, ultrasonic devices use acoustic cavitation to remove dirt and contaminants from objects immersed in a liquid.

Laser-induced cavitation: It is a type of cavitation that is produced through depositing high amounts of energy into the liquid locally even if without the presence of initial nuclei. When a laser is directed onto a specific point in a liquid, it can induce an optical breakdown, resulting in the formation of a plasma. As the plasma expands, it creates a cavity in the form of a single vapour bubble within the liquid. With precise control, it is possible to generate an isolated spherical bubble. Although the process of generating laser-induced bubbles differs from other technical devices, the behavior of these bubbles is similar. This technique enables the study of individual bubbles in well-defined environments, providing valuable insights into the physics of isolated bubble dynamics. Another similar way of generating such a cavitation bubble is by an electrical discharge through a spark.

Oscillatory cavitation: The cavitation caused by a series of continuous high-frequency and high-amplitude pressure fluctuations in the liquid is called oscillatory cavitation. The word "oscillatory" is used because the oscillating pressure field is generated by the oscillation of a solid surface immersed in the liquid along its normal direction. Cavitation around the cooling jacket of a diesel engine is a typical example. In addition, the cavitation on the surface of the acoustic sensor also belongs to the oscillatory cavitation.

Hydrodynamic cavitation: It is the most common and important case encountered in engineering applications. Hydrodynamic cavitation is caused by low pressure associated with flow dynamics, such as flow acceleration, flow separation and strong vortical motions. Hydrodynamic cavitating flows are usually described with a characteristic number termed cavitation number σ that indicates the cavitation intensity. The general definition is given by $\sigma = (P_\infty - P_{\text{vap}})/\,(0.5\rho_\infty u_\infty^2)$, where P_∞, ρ_∞ and u_∞ are free stream pressure, density and velocity respectively. Although other scale effects might influence cavitation, similar cavitation conditions can generally be achieved for the same cavitation number. A low cavitation number indicates a higher likelihood of cavitation initiation and a larger volume of vapour formation.

Hydrodynamic cavitation can take different forms depending on how the low-pressure regions are generated, and they can be divided into three groups:

- Travelling bubble cavitation. Individual bubbles arise from regions of cavitation inception as a result of rapid growth of cavitation nuclei. They are first transported by the flow and then implode when they reach zones of high pressure.
- Attached cavitation. It appears in a low-pressure separated region close to the solid surface. The typical flow scenarios are cavities

forming on the suction side of a hydrofoil or an impeller blade. If the length of the attached cavity exceeds the body upon which it develops, it is called super cavitation, otherwise it is termed as partial cavitation.

- Vortex cavitation. The fluid in the cores of vortices is prone to vapourizing due to low pressures prevailing there. It is commonly observed at the tips of propeller blades or in the free shear layers where Kelvin-Helmholtz vortices can develop.

1.4. Advantages and Disadvantages of Cavitation

Cavitation has its advantages and disadvantages, depending on the application and context. Here are some of the key advantages and disadvantages of cavitation:

Advantages:

- Energy Transfer and Mixing: Cavitation generates shock waves and high-speed liquid jets during bubble collapse, promoting fluid mixing and enhancing reaction efficiency in certain applications.
- Acoustic Applications: Cavitation can be induced by acoustic waves, finding wide applications in fields such as medicine (e.g., ultrasound therapy) and other industries.
- Material Processing: Cavitation can be used for material removal, cutting, and surface modification, such as in ultrasonic cleaning or laser ablation.
- Cooling: In some cases, cavitation can be harnessed for cooling by absorbing heat through bubble collapse.

Disadvantages:

- Material Wear: The collapse of cavitation bubbles generates shock waves, microjets, and high local temperatures. This collapse and

subsequent implosion of bubbles can cause erosion, pitting, and damage to nearby surfaces.

- Noise and Vibration: Cavitation can produce noise and vibrations, which may interfere with equipment operation and cause damage.
- Reduced Efficiency: In certain situations, cavitation can lead to decreased equipment performance, such as reduced efficiency in water pumps and turbines.
- Fluid Dynamics Issues: Cavitation can induce unstable flow patterns and vortices, negatively impacting fluid dynamics systems.

In summary, the advantages and disadvantages of cavitation depend on its management, control, and optimization in specific applications. Engineers and researchers strive to harness the advantages of cavitation while minimizing or mitigating its disadvantages to ensure safe and efficient operation in various industries and systems.

1.5. Sheet and Cloud Cavitation

Generally speaking, partial cavities have two forms of appearance as well in case of internal flows (in a Venturi) as in case of external flows (on a hydrofoil).For small incident angles (hydrofoil - angle of attack; Venturi - divergent and convergent angles) and high free-stream cavitation numbers, the attached cavity appears to be stationary at a fixed location, and the observed cavity length is rather constant. This situation is referred to as sheet cavitation. A typical sheet cavitation forming on the suction side of a hydrofoil or on the divergent wall of a Venturi channel is presented in **Figure 1.2**. When the cavitation number is decreased or/and the incident angle is increased to a certain extent, the stable sheet cavity cannot be sustained. A large portion of the cavity is shed periodically from the main cavity forming a cloud-like structure in the cavity wake, and as a result the cavity length undergoes significant oscillations. This phenomenon is

commonly called cloud cavitation. **Figure 1.3** shows two examples of cloud shedding.

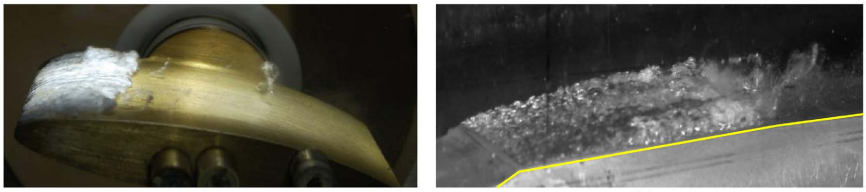

(a) (b)

Figure 1.2. (a) Sheet cavitation on the suction side of a hydrofoil from Foeth (2008b); (b) sheet cavitation on the divergent wall of a Venturi channel from Barre *et al*. (2009).

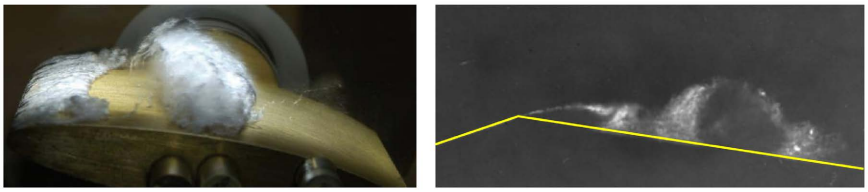

(a) (b)

Figure 1.3. (a) Cloud cavitation on the suction side of a hydrofoil from Foeth (2008b); (b) cloud cavitation on the divergent wall of a Venturi channel from Stutz & Reboud (1997a).

Although cavitation is inherently unsteady, sheet cavitation is usually stated to be stable or quasi-stable since the shedding of small vapour-filled vorticesis confined in the cavity closure region, whose characteristic length scale is much smaller than the whole cavity length. Sheet cavitation is sometimes described to be an open cavity due to its frothy appearance at the closure as classified by Laberteaux & Ceccio (2001a). In contrast, cloud cavitation results in large fluctuations of cavity volume and thus is stated to be unstable. The violent collapse of the shed cloud in the downstream wake region can emit pressure waves of high amplitude, which is considered as the main

source of noise and erosion (Reisman *et al*. 1998; Dular *et al*. 2015). Therefore, cloud cavitation is much more destructive than a stable sheet cavity.

1.6. Mechanisms for Sheet-to-Cloud Cavitation Transition

In a classical point of view, the different behaviors of a partial cavity depend on the existence or absence of re-entrant flow originating from a stagnation point behind the cavity closure.

As for sheet cavitation (open partial cavities), Gopalan & Katz (2000), Callenaere *et al*. (2001) and Laberteaux & Ceccio (2001a) concluded that no clear re-entrant jet or only the weak reverse flow existed at the trailing edge of the cavity due to weak adverse pressure gradient. Leroux *et al*. (2004) did not detect a clear sign of a pressure wave traveling from the cavity closure towards the leading edge inside a stable sheet cavity through ten aligned pressure transducers flush-mounted along the suction side of a hydrofoil, and they attributed it to the absence of the re-entrant jet. Barre *et al*. (2009) measured a clear re-entrant flow in a globally-steady sheet cavitation using a double optical probe technique. However, in their simultaneous numerical simulation, the re-entrant jet was not predicted, and eventually they did not further clarify the role played by the re-entrant jet in stable sheet cavitation. In general, the absence of re-entrant flow was regarded as the main reason for the stable flow regime of sheet cavitation.

The periodic shedding of large cloud was observed firstly by Knapp (1955) and he proposed a re-entrant jet model to explain the transition from stable sheet cavitation to periodic cloud cavitation. This re-entrant jet mechanism is presented schematically in **Figure 1.4**. As the attached cavity grows to a certain length, a thin re-entrant jet, mainly composed of liquid, forms near the cavity closure region

and moves upstream beneath the cavity. When this jet reaches the cavity leading edge, the whole cavity is pinched off forming a rolling cavitation cloud that is then convected downstream by the main flow until it collapses. Meanwhile a new cavity begins to grow again and the entire process is repeated.

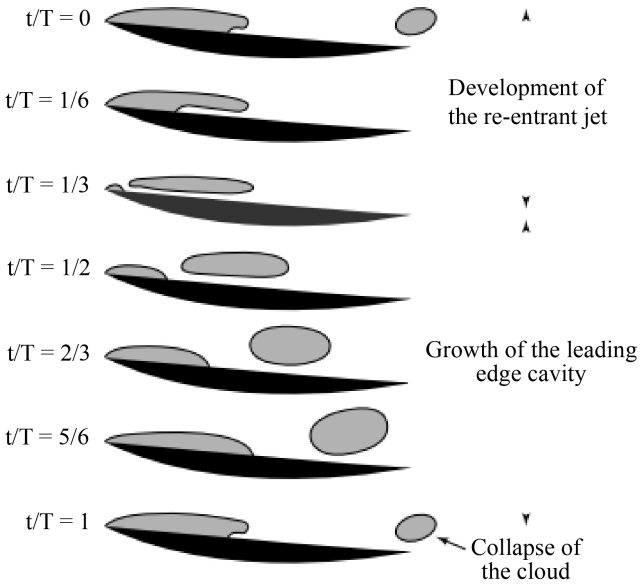

Figure 1.4. Typical unsteady behavior of a partial cavity with the development of a re-entrant jet and the periodic shedding of cavitation clouds from Franc & Michel (2005).

After the establishment of the re-entrant jet model, many studies have been conducted in order to verify the existence, development, the correlation of re-entrant jet with cavitation dynamics. Furness & Hutton (1975) predicted the development of re-entrant jet using a potential flow model. The injection of ink was used by Le *et al*. (1993) to visualize the re-entrant flow, and the ink was observed near the leading edge, confirming an upstream flow component. Kawanami *et al*. (1997) placed a small obstacle on the suction side of a hydrofoil to

prevent the re-entrant jet from moving upstream, and the large cloud shedding was not observed in the experiment, demonstrating the re-entrant jet was the primary cause of cloud cavitation. Pham *et al*. (1999) placed a series of six electrical impedance probes spaced equally on the upper flat surface of the hydrofoil to detect the liquid front corresponding to the re-entrant jet. They found that the mean velocity of the re-entrant jet attained a maximum value near the cavity closure region and was of the same order of magnitude as the free stream velocity. Laberteaux & Ceccio (2001b) observed that ageometry with spanwise variation can sustain stable cavities with re-entrant flow since the re-entrant flow was directed away from the cavity. The conditions necessary for the development of the re-entrant jet has been explored by Callenaere *et al*. (2001). They confirmed the critical role of the adverse pressure gradient at the cavity closure in the onset of the re-entrant jet instability.

In the numerical simulation of cloud cavitation, the RANS models generally overestimate the turbulent viscosity in the rear part of the cavity. The re-entrant jet is consequently stopped too early and it does not result in any cavity break off. Coutier-Delgosha *et al*. (2003) reproduced the periodic cloud shedding in a Venturi-type section by using a correction initially proposed in Reboud *et al*. (1998) on turbulent viscosity which actually reduces the friction losses that the re-entrant jet encounters. Pelz *et al*. (2017) introduced a physical model of transition from sheet to cloud cavitation based on the criterion that the transition occurs when the re-entrant jet reaches the point of origin of the sheet cavity. A good agreement was found between the model-based calculations and the experimental measurements. Their numerical work could also demonstrate the importance of re-entrant jet to initiate cloud cavitation.

In addition to the classical re-entrant jet, the mechanism of con-

densation shock waves dictating sheet-to-cloud shedding has been widely acknowledged in recent years. As early as 1964,the occurrence of condensation shocks in cavitating flows was speculated by Jakobsen (1964) based on the fact that the sound speed in a two-phase mixture is significantly lower than that in either component, *i.e.* water or water vapour (Brennen 1995). However, the direct experimental observation was made only recently by Ganesh *et al.* (2016). As shown in **Figure 1.5**, using X-ray densitometry to visualize the instantaneous distribution of vapour volume fraction in the cavitating flow over a wedge, they found that the leading edge cloud shedding at lower cavitation numbers was resulted from an upstream propagating void fraction discontinuity, *i.e.* a condensation shock front. In order to demonstrate this new finding different from the classical re-entrant jet mechanism, Ganesh *et al.* (2017) also

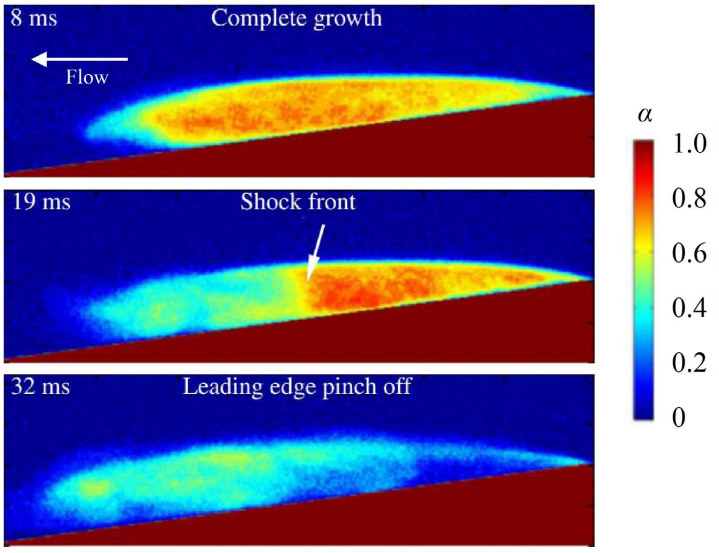

Figure 1.5. Instantaneous void fraction fields illustrating the condensation shock mechanism to cause sheet-to-cloud cavitation from Ganesh *et al.* (2016).

placed a small obstacle under the sheet cavity just like what Kawanami *et al*. (1997) did. The results showed that cloud shedding in the case of condensation shocks cannot be prevented since the condensation front spans the entire cavity height rather than near the wall only.

Motivated by the pioneering work of Ganesh *et al*. (2016), many interesting numerical and experimental studies were performed later towards revealing the condensation shock mechanism in different configurations (e.g. Wu *et al*. 2017; Jahangir *et al*. 2018; Budich *et al*. 2018; Wu *et al*. 2019; Trummler *et al*. 2020; Bhatt & Mahesh 2020). In agreement with the original experiment, all these works found that with a sufficient reduction of the cavitation number, condensation shocks overtaking re-entrant jets became the dominant mechanism for large-scale cloud shedding. Nevertheless, they had divergence on the cause for the onset of condensation shock. In the PhD thesis of Ganesh (2015), it was described that a rapid growth in cavity length and vapour content, hence reduced speed of sound and increased compressibility, resulted in the production of shock waves at the rear of the cavity. Wu *et al*. (2017), Jahangir *et al*. (2018) and Bhatt & Mahesh (2020) observed that the propagation of condensation shocks was triggered by the impingement of collapse-induced pressure waves from previously shed clouds. This was also found by Budich *et al*. (2018), but in addition they also captured the initiation of condensation shocks in the absence of cloud collapsing. It implied that both the rapid cavity growth and the collapse-induced pressure wave could contribute to the formation of overpressure behind the cavity which was sufficient to induce a condensation shock front. It should be noted that a pressure wave with high amplitude emanating from a large cloud collapse might crush the growing cavity suddenly as described by Leroux *et al*. (2004, 2005), which was different from the propagation of condensation shock through the cavity.

1.7. Studies on Cavitation-Turbulence Interactions

The cavitation dynamics is also strongly related to the cavitation/ turbulence coupling: the effect of cavitation (including formation and collapse of vapour cavities) on turbulence has been investigated numerically and experimentally.

As for the numerical aspect, Dittakavi *et al*. (2010) used large eddy simulation (LES) to predict cavitating flows in a Venturi nozzle. By comparison of three cases at different cavitation numbers, they concluded that the vapour formation due to cavitation suppressed turbulent velocity fluctuations and the collapse of vapour structures in the downstream region was a major source of vorticity production, resulting in a substantial increase of turbulent kinetic energy. Xing *et al*. (2005) observed, in their numerical simulation of vortex cavitation in a submerged jet, that cavitation suppressed jet growth and decreased velocity fluctuations within the vapourous regions of the jet. Gnanaskandan & Mahesh (2016) investigated partial cavitating flows over a wedge and found that the streamwise velocity fluctuations dominated the other two components within the cavity, while all three components of fluctuations were equally significant near the cavity closure and downstream of the cavity,

Regarding the experimental aspect, the acquisition of quantitative velocity fields mainly relied on PIV measurements. Gopalan & Katz (2000) and Laberteaux & Ceccio (2001) observed the largest turbulent fluctuations in the region downstream of the cavity which were regarded as the impact of vapour collapse. Iyer & Ceccio (2002) investigated the effect of developed cavitation on the flow downstream of the cavitating shear layer. They found that the collapse of vapour bubbles led the streamwise velocity fluctuations to be increased but the cross-stream fluctuations and the Reynolds shear stress to be decreased. Aeschlimann *et al*. (2011b) performed velocity measure-

ments in a 2D cavitating shear layer. They observed that a complex combination of the production of vapour bubbles coupled with their collapse added additional velocity fluctuations, mostly in the main flow direction, while the turbulent shear stresses almost remained constant.

1.8. A Review of Measurement Techniques for Cavitating Flows

Detailed flow measurements are essential for the understanding of cavitating flows. Due to the existence of non-transparent liquid/vapour mixtures, visual observation by a fast speed camera (high speed photography) is the most straightforward and widely-used method to capture the temporal evolution of cavitation structures, thereby providing insight into the underlying physics (Foeth *et al*. 2008a; Aeschlimann *et al*. 2012). Through post-processing of the high speed video images, it is possible to derive some quantitative data, such as the cloud shedding frequency and the cavity growth rate (Prothin *et al*. 2016; Jahangir *et al*. 2018). Synchronized with dynamic pressure measurements, high speed images can also reveal the pressure change associated with the cavity unsteady behaviors (Wang *et al*. 2017; Wu *et al*. 2017). On one hand, cavitation visibility helps to obtain its global flow characteristics. On the other hand, cavitation opacity hinders the measurements inside the two-phase region. In order to analyze the internal flow structures of cavitation, other techniques, able to visualize the two-phase morphology as well as measure quantitative data on void fraction and velocity, are required.

1.8.1. Local Measurements by Intrusive Probes

Ceccio & Brennen (1991) detected individual vapour bubbles using a network of silver electrodes mounted on the surface of a hydrofoil, and thus acquired their velocities. Stutz & Reboud (1997a; 1997b;

2000) used a double optical probe to measure the time-averaged void fraction and vapour-phase velocity inside the cavity generated in a two-dimensional Venturi-type section. In this technique, the local velocity was estimated by the time interval of a bubble passing two probe tips successively and the local void fraction was defined as the ratio of the cumulated time of vapour phase at the tip of the probe to a given time of observation. In spite of a relative large measurement uncertainty of about 15%, their work gave a preliminary description of the two-phase flow structure inside a sheet cavity and confirmed the presence of a reverse flow along the solid surface. Coutier-Delgosha *et al*. (2006) made the first attempt to visualize the two-phase morphology inside the sheet cavity by means of a new endoscopic device. Based on the observation at different stations along the hydrofoil chord, they found that the internal structure close to the leading edge was characterized by large vapour bubbles with a similar critical size and then they were rapidly split into smaller bubbles downstream; most of the bubbles do not have a spherical shape.

1.8.2. Particle Image Velocimetry (PIV)

Different from intrusive and pointwise measurements using probes, PIV enables a whole-field acquisition of instantaneous velocity vectors with little perturbation on the flow. It has thus been applied to a wide range of fluid flows, but in cavitating flows, the strong scattering and reflection from the liquid/vapour mixture will obscure the scattering light from the surrounding tracer particles. This contaminating effect on the PIV measurements can be avoided by injecting laser-induced fluorescent (LIF) particles which emit light with different wavelength from the laser. The reflected and scattered light, at the wavelength of the laser, is blocked by the optical filter mounted in front of the lens and only the light emitted by the particles is recorded by the camera. However, if there are many vapour bubbles

passing between the laser sheet and the camera, the optical paths starting from the fluorescent particles will be deviated severely or blocked completely. As a consequence, most PIV-LIF measurements have focused on the liquid flow regions outside the cavity (Laberteaux & Ceccio 2001; Foeth *et al*. 2006; Kravtsova *et al*. 2014) or turbulent cavitating regions with low void fraction (Iyer & Ceccio 2002; Aeschlimann *et al*. 2011b). Interestingly, the work of Dular *et al*. (2005) shows that if the position of the laser sheet was close enough to the observation window (~5 mm), the detected particles would be sufficient to evaluate the velocity field inside the sheet cavity. However, the measured velocity field is not representative since it is strongly subjected to the wall effects.

1.8.3. X-Ray Densitometry Based on Absorption Contrast

Both X-rays and visible light are, in nature, part of the electromagnetic spectrum. However, due to having a much shorter wavelength than visible light, X-rays can penetrate most optically opaque media with weak interactions. This distinct advantage makes X-ray radiography a powerful method to visualize opaque multiphase flows (Heindel 2011).

For cavitating flows, X-ray radiography can be used to measure local void fraction, *i.e*. density because of the absorption difference between water and vapour. Stutz & Legoupil (2003) applied firstly the X-ray densitometry to cloud cavitation formed in a Venturi-type test section. They found that the mean void fraction varies regularly from 25% at the upstream end of the mean cavity to 10% in the downstream part. Coutier-Delgosha *et al*. (2007) performed void fraction measurements of cavitation on a plano-convex hydrofoil using the same X-ray attenuation device. They reported that the local mean vapour volume fraction does not exceed 35 % for small sheet cavities, and 60% for the large ones. Another application of X-ray attenuation

measurements can be found in Aeschlimann *et al*. (2011a) where the main vortex shedding frequency in a turbulent cavitating shear layer was estimated through spectral analysis of the void fraction signal. In recent works (Ganesh *et al*. 2016; Wu *et al*. 2019), time-resolved X-ray densitometry was used to measure the instantaneous distribution of void fraction in the cavitating flow field. A well-defined void-fraction discontinuity spanning the thickness of the cavity was observed to propagate upstream. According to the authors, this discontinuity represented a bubbly shock front which was responsible for periodic shedding of large-scale vapour clouds.

A standard 2D X-ray densitometry system can only provide a projection of the sample's density distribution in the direction of the X-ray beam. This means that the 3D flow information is collapsed onto a single 2D plane. As a remedy, the actual 3D spatial distribution can be retrieved using a tomographic reconstruction. The examples of using X-ray computed tomography (CT) to measure the radial distribution of void fraction in circular nozzle cavitating flows can be found in Bauer *et al*. (2018) and Jahangir *et al*. (2019).

1.8.4. X-Ray Velocimetry Based on Phase Contrast

X-ray phase-contrast imaging enables clear visualization of boundaries between phases with different refractive index (Kastengren & Powell 2014). Aside from detailed illustration of two-phase morphology (Karathanassis *et al*. 2018), X-ray phase-contrast images can also be used to perform velocimetry by tracking either seeded particles or phase interfaces. Early applications of X-ray velocimetry are for solving the so-called optical access issue. For example, Lee & Kim (2003) employed a low-energy synchrotron X-ray beam instead of a laser sheet to illuminate the seeded particles in the flow in an opaque tube. The instantaneous velocity field was extracted by cross-correction similar to the conventional PIV analysis. For opaque flows with a

very low speed (a few millimeters per second), they also developed a compact X-ray-based PIV system employing a medical X-ray tube as a light source (Lee *et al*. 2009).

For high speed fluid flows, a short exposure time is needed to freeze the fluid motion. The third-generation synchrotron radiation sources such as the advanced photon source (APS) at Argonne National Lab can produce a high-energy and coherent X-ray beam which satisfies the requirements of ultra-fast X-ray phase-contrast imaging. Im *et al*. (2007) used the APS X-ray source to greatly improve the particle image quality making single-particle tracking velocimetry possible in an optically opaque vessel. Wang *et al*. (2008) revealed for the first time the internal structures of high-speed (order of 60 m/s) optically dense sprays near the nozzle exit using the ultrafast APS X-ray phase-contrast imaging technique. The velocity fields were measured by tracking the movements of the phase enhanced liquid-gas boundaries. A similar application of synchrotron X-ray phase-contrast imaging in fuel injector nozzles was presented by Moon (2016) for comparing the dynamic structure of biodiesel and conventional fuel sprays.

The first attempt to measure velocity field inside cavitating regions by means of fast X-ray image was described by Coutier-Delgosha *et al*. (2009). Later Khlifa *et al*. (2017) also used the similar method to measure high speed cavitating flows in a small size Venturi-type test section. In the experiment, the flows were seeded with silver-coated hollow glass sphere particles which were visualized clearly along with the bubbly structures of cavitation by combined effects of X-ray absorption and phase contrast enhancement. Cross-correlation algorithms were applied on the particles and the bubble structures to evaluate the liquid-phase and the vapour-phase velocities respectively. Furthermore, the distribution of vapour volume fraction was

determined from X-ray absorption difference in vapour and liquid. Based on the experimental results, the presence of significant slip velocities between the liquid and vapour phase was demonstrated quantitatively for the first time. Their work laid a foundation for the present study on flow structures and dynamics inside sheet cavities.

1.9. Outline of the Book

Although cavitation has been investigated extensively for more than a century, a full understanding of the physical processes underlying the cavitating flows is still far from being realized at the present time. This is mainly due to the lack of quantitative experimental data on two-phase structures and dynamics of cavitation. Therefore, high-fidelity and detailed measurements of cavitating flow fields, especially in the opaque diphasic mixture areas, are extremely desired for a better knowledge of the physical mechanisms governing the cavitation instabilities. This will help to deduce effective means for controlling the negative consequences of cavitation and increasing its positive influence. Furthermore, the quantitative experimental data can be used to validate and improve the numerical simulation models for cavitation. Once reliable predictions are achieved, the costs and time concerning cavitation tests will be reduced substantially.

This book is composed of the following 7 chapters. Chapter 2 provides a brief description of the experimental setup and the fast X-ray imaging technique. The emphasis of this chapter is put on the procedures from visualizations to velocity and void fraction field measurements in cavitating flows. In Chapter 3, the complex two-phase flow structures inside the sheet cavity are revealed in detail based on the data from the X-ray measurements. Chapter 4 deals with a comparative study of sheet cavitation at three stages (the early stage, intermediate stage and developed stage). The comparison shows the effect of re-entrant jet behaviors on sheet cavity structures and dy-

namics. The influence of cavitation on turbulent fluctuations is also discussed. Chapter 5 analyzes the cavitating flows in a Venturi channel with side gaps. It is found that cloud cavitation can be suppressed by altering the propagation path of the re-entrant jet. In Chapter 6, three mechanisms (*i.e*. re-entrant jet mechanism, condensation shock mechanism and collapse-induced pressure wave mechanism) to initiate cloud cavitation are described in detail, and the reasons causing the scale effect on Venturi cavitating flows are discussed. Chapter 7 deals with the thermodynamic effects of cavitation in hot water. A comparative study of sheet cavitation at different temperatures shows that the thermal effect has a significant impact on the cavity size and shedding dynamics of sheet cavity structures. The book is ended with a general conclusion in Chapter 8 summarizing the main contributions of this work and several perspectives for future research are proposed.